Mössbauer spectroscopy of ^{119}Sn from implantations of radioactive ^{119}Sb in metals

H. Muramatsu* and T. Miura
National Laboratory for High Energy Physics, Tsukuba-shi, Ibaraki-ken 305, Japan

H. Nakahara
Department of Chemistry, Faculty of Science, Tokyo Metropolitan University, Setagaya-ku, Tokyo 158, Japan
(Received 27 November 1989)

Mössbauer emission spectra of ^{119}Sb-implanted metal sources prepared by means of an isotope separator have been measured for the 23.87-keV transition of ^{119}Sn. Spectra of the implantations into β-Sn, Au, Pt, and Al showed almost a single resonance line attributable to substitutional sites; in the case of Pb and Y, however, complex spectra were observed. These observations were compared with the data obtained previously from ^{119m}Sn implantations in terms of the decay characteristics. From Mössbauer fraction measurements impurity-host force-constant ratios for ^{119}Sn were determined by using Mannheim's impurity-lattice theory in several face-centered-cubic metal hosts.

I. INTRODUCTION

At present, the ion-implantation technique by means of isotope separators is utilized not only as a doping method in semiconductor technology, but also as a superior experimental method in solid-state physics and chemistry. Mössbauer spectroscopy combined with this technique, i.e., Mössbauer emission spectroscopy on γ radiation from radioactive isotopes implanted as probe atoms into solids, is of particular importance for the study of the electronic structure and vibrational properties of atoms introduced as an impurity. Among the parameters obtained from Mössbauer measurements on implanted nuclei, the isomer shift gives information of the electronic state of the implanted atoms, and the recoilless fraction as well as the second-order Doppler shift are related to the mean-square displacement or velocity. These parameters are determined from the spectral analysis with a least-squares fitting method. From such experiments, we can get information on implantation problems such as the lattice location of implanted atoms. They are also applicable to a surface analysis of the materials.[1]

In the present work, radioactive ^{119}Sb, which decays to the first excited state of ^{119}Sn by orbital electron capture, has been implanted into several metal hosts by an electromagnetic isotope separator in order to investigate the behavior of the implanted atoms by Mössbauer spectroscopy. Mössbauer studies of the implantation of the nuclides with $A=119$ have been reported by Weyer and his co-workers for many cases, that is, implantations of radioactive precursors to the Mössbauer nucleus ^{119}Sn in elemental group IV and III–V compound semiconductors and in fcc and other metals. Since our results for the case of stannous compounds were already reported,[2] in this paper our attention is almost entirely focused on implanted ^{119}Sb in several metals comparing our data with the data obtained by the Aarhus group in ^{119m}Sn implantations.[3,4] Therefore, we describe the behavior of the ^{119}Sn isomer shift for ^{119}Sb implanted as an impurity parametrizing some physical properties of host materials, the difference of the implantation behavior due to the different precursors and impurity-host force-constant ratios derived from the analysis of Mössbaur measurements.

II. EXPERIMENTAL

The ^{119}Sb ($T_{1/2}=38.0$ h) activity was obtained by milking a ^{119m}Te ($T_{1/2}=4.7$ d) source. The latter was produced by bombarding natural Sb metal with 38-MeV protons from the azimuthally varying field cyclotron of Tohoku University with a beam current of about 15 μA for several hours. The target (1.5 g/cm^2) was dissolved in aqua regia which contained a 10-mg tellurium carrier. The tellurium was reduced and precipitated from 6N HCl by adding hydrazine and sodium sulfite solution in order to separate from antimony. The metallic tellurium was dissolved in 6N HCl which contained a 2-mg antimony carrier. After standing for 2 or 3 d for the daughter nuclide ^{119}Sb to build up, the ^{119}Sb was precipitated from a 3N HCl solution with hydrogen sulfide, and only the antimony sulfide was dissolved in concentrated HCl. The antimony was electrodeposited on platinum wire (25 μm in diameter) from a 4N HCl solution and mounted in the ion source of the isotope separator. Further milking of ^{119}Sb was performed after a new growth period.

Implantation of ^{119}Sb was carried out at the terminal voltage of 20 kV at room temperature by means of the electromagnetic isotope separator of the Cyclotron and Radioisotope Center, Tokohu University.[5] The dose rate was $0.9-3\times10^7$ atoms/cm^2 s for the mass number 119, and the number of implanted ^{119}Sb atoms was determined to be $0.7-2\times10^{12}$ atoms/cm^2 from the radioactivity of the implanted samples. The ^{119}Sb ions were implanted in a region of about 10 mm in diameter. The hyperpure metallic foils or plates (Al, Y, β-Sn, Pt, Au, and Pb) as host materials were mechanically polished to make the surface fresh and were washed with acetone. In order to keep these foils or plates from oxidizing, they were put in a vacuum desiccator until just before the implantation.

The Mössbauer spectra were measured with a conventional electromechanical transducer operating in a constant acceleration mode. The temperature of the sources was kept at the two measuring temperatures, namely, 78

K and 150 or 200 K. The absorber was a powdered $CaSnO_3$ containing about 1 mg/cm^2 ^{119}Sn, which was kept at 78 K in every measurement. The 23.87-keV Mössbauer γ rays were detected with a pure germanium low-energy phonon spectrometer having an active volume of 5 cm^3. The velocity calibration of the drive was performed by measuring peak positions of an enriched iron metal foil. The zero-velocity point of the drive was determined from the absorption spectra measured with a $CaSnO_3$ absorber and a standard $Ca^{119m}SnO_3$ source. The measured spectra were analyzed by means of a least-squares fit computer code SALS.[6]

For some of the implanted samples postannealing was carried out in a quartz-tube furnace with flowing dry and oxygen-free argon at 1 atm. The samples were cooled down to room temperature in argon atmosphere. In most cases the radioactivity of the sample was slightly reduced after annealing.

III. EXPERIMENTAL RESULTS AND DISCUSSION

A. Site assignment of implanted atoms

1. Implantation into β-Sn

Figure 1 shows Mössbauer spectra measured without surface treatment before implantation, that is, the surface of β-Sn was not polished mechanically. The four Mössbauer spectra correspond to those observed without annealing, with annealing at 150 °C for 15 min, at 150 °C for 60 min, and at 200 °C for 60 min, respectively. All were measured at liquid-nitrogen temperature. All four spectra can be consistently analyzed by decomposition into four lines. Such a decomposition procedure is often problematic if no additional information on the number of lines is obtainable. In this case, since no good fit was obtained with two lines, it seemed reasonable to assume that four lines existed in the spectrum. In the analysis the positions of the two lines having larger intensities were loosely fixed and their linewidths were made to be almost equal to each other. If two lines at $\delta=3.6$ mm/s and 1.8 mm/s form a quadrupole doublet, it is reasonably understood that they were attributed to SnO arising from implantations into the oxidized surface layer of the tin foil. The isomer shift for this site was found to be $\delta=2.7$ mm/s, which is in good agreement with previous Mössbauer studies.[7-9] The values of isomer shift and quadrupole splitting reported previously are $\delta=2.68$ mm/s, $\Delta=1.33$ mm/s from Ref. 7, $\delta=2.71$ mm/s, $\Delta=1.45$ mm/s from Ref. 8, and $\delta=2.8$ mm/s, $\Delta=1.6$ mm/s from Ref. 9 for tetragonal SnO, and $\delta=2.58$ mm/s, $\Delta=1.99$ mm/s from Ref. 7, $\delta=2.60$ mm/s, $\Delta=2.20$ mm/s from Ref. 8, and $\delta=2.7$ mm/s, $\Delta=2.2$ mm/s from Ref. 9 for orthorhombic SnO, respectively. In the present case, although the quadrupole splitting tends to decrease from a no-annealing sample (1.97 mm/s) to a 200 °C annealing sample (1.57 mm/s), which is somewhat larger than the reported values for tetragonal SnO, this may be due to the imperfect formation of the SnO-like species or to surroundings around these species slightly different from the normal SnO lattice. As is well established,[2,10,11] the line at $\delta=2.5$ mm/s originates from the normal substitutional sites in β-Sn. The residual line at zero velocity was attributed to SnO_2 formed in the surface-oxide layer.[2,11] These observations imply that Mössbauer spectroscopy is a useful tool for studying the surface properties of materials after ion implantation. Since the implantation energy of 20 keV in this work is enough to implant Sb atoms into the tin layers of 7 μg/cm^2 (96 Å) in depth,[12] the observed Mössbauer spectra indicate that tin foils left in air for a long time are oxidized up to such a depth from the surface. The annealing behavior of sources of ^{119}Sb implanted into these β-Sn foils are relatively simple as shown in Fig. 2, that is, only the intensity of line 2 decreases with increasing annealing temperature. As mentioned earlier, line 2 is attributed to the normal substitutional sites of the β-tin lattice. The decrease of line 2 may be due to the

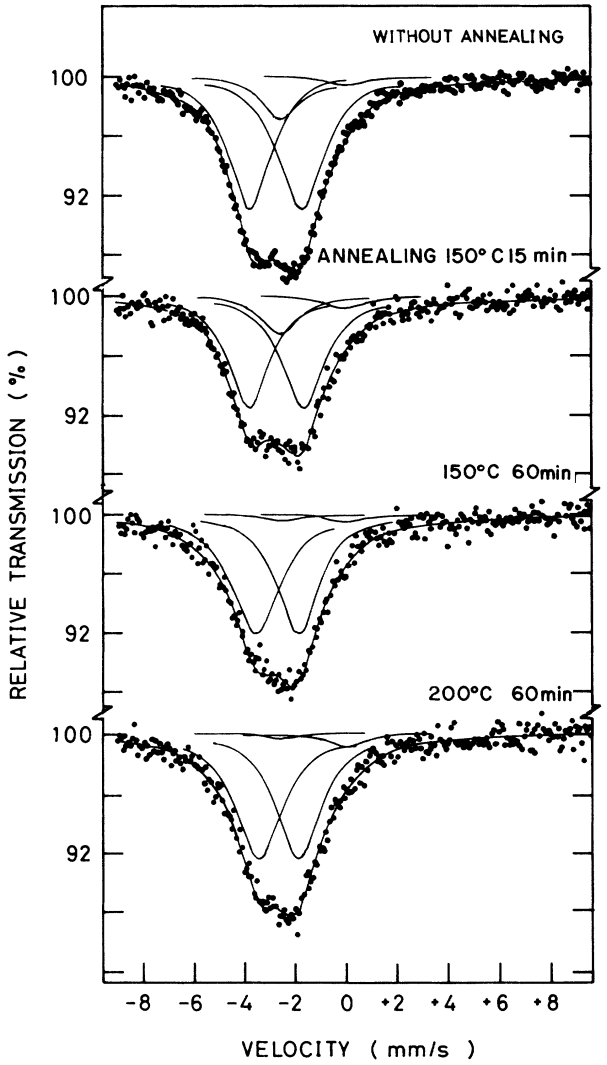

FIG. 1. Mössbauer spectra obtained from sources of ^{119}Sb implanted into β-Sn without surface treatment before implantation. The spectra were measured with a $CaSnO_3$ absorber at liquid-nitrogen temperature under various annealing conditions.

diffusion of tin atoms to the oxide layer on the surface, as has been pointed out previously.[4,13]

The implantation was also performed using a matrix which was mechanically polished to be free from an oxidized surface layer. In Fig. 3 two Mössbauer spectra measured at 200 K and at liquid-nitrogen temperature are shown. Clearly, the spectra were fitted by single lines. The single line at $\delta=2.48$ mm/s is attributable to the normal substitutional site in the host lattice since the result from this sample was in good agreement with the data[14] from samples prepared by a diffusion method and with the result from a transmission measurement with $Ca^{119m}SnO_3$ source. Results for the analyses of the ^{119}Sb implantation into β-Sn are given in Table I.

We used the Debye model in analyzing the temperature dependence to deduce the recoilless fraction, i.e., the Debye-Waller factor (f) is expressed by the following equation:

$$f=\exp\left\{-\frac{6E_R}{k\Theta}\left[\frac{1}{4}+\left[\frac{T}{\Theta}\right]^2\int_0^{\Theta/T}\frac{u\,du}{e^u-1}\right]\right\}, \quad (1)$$

where E_R is the recoil energy of the Mössbauer atom, Θ is the characteristic Debye temperature of the host. T is the absolute temperature, and k is Boltzmann's constant. At high temperatures, Eq. (1) can be approximated by[15]

$$f=\exp[-y(4/x+x/9)], \quad (2)$$

where $x=\Theta/T$ and $y=3E_R/2k\Theta$. In the temperature range of $\Theta=50-500$ K and $T>78$ K, Eq. (2) is a good approximation of Eq. (1) with a relative accuracy of

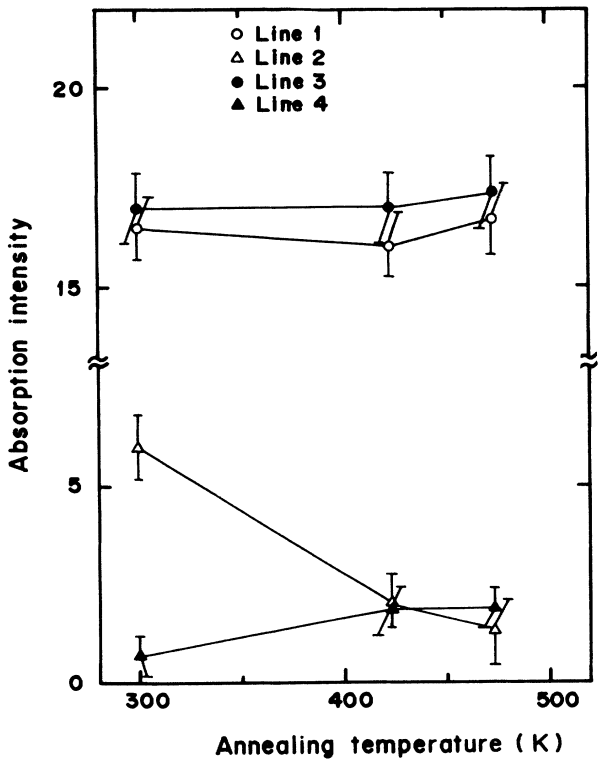

FIG. 2. Absorption intensities as a function of annealing temperature for the lines found in the spectrum from the source implanted into β-Sn without surface treatment before implantation.

TABLE I. Results of Mössbauer measurements on ^{119}Sb implanted into β-Sn.

Sample	T_{meas} (K)	Line 1			Line 2			Line 3			Line 4		
		δ (mm/s)	I (%)	Γ (mm/s)	δ (mm/s)	I (%)	Γ (mm/s)	δ (mm/s)	I (%)	Γ (mm/s)	δ (mm/s)	I (%)	Γ (mm/s)
No anneal.	78	3.65(4)	8.71(31)	1.90(6)	2.51(7)	3.11(40)	1.92(7)	1.68(4)	8.82(34)	1.93(7)	0.01(7)	0.35(27)	1.94(8)
No anneal.	300	3.69(7)	1.72(26)	1.95(7)	2.50(7)	0.45(34)	1.95(7)	1.66(7)	1.71(30)	1.95(7)	0.00(7)	0.46(16)	1.95(7)
Anneal. 150°C 15 min	78	3.69(4)	6.92(29)	1.87(7)	2.51(7)	2.59(39)	1.91(7)	1.61(4)	7.29(33)	1.90(7)	0.01(7)	0.32(27)	1.94(7)
Anneal. 150°C 60 min	78	3.55(4)	7.83(31)	2.05(7)	2.50(7)	1.01(41)	1.95(7)	1.84(4)	8.44(35)	2.01(7)	0.02(7)	0.96(26)	1.95(7)
Anneal. 200°C 60 min	78	3.43(4)	8.31(33)	2.01(7)	2.50(7)	0.65(41)	1.95(7)	1.86(4)	8.77(35)	1.98(7)	0.03(7)	0.97(26)	1.95(7)
Polished	78				2.48(2)	14.46(31)	1.47(5)						
No anneal.	200				2.47(5)	4.63(24)	1.69(8)						

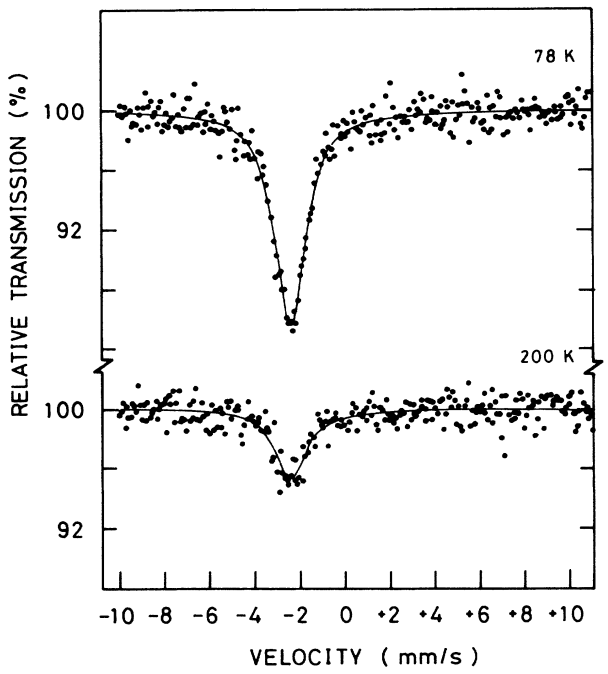

FIG. 3. Mössbauer spectra obtained from the source of ^{119}Sb implanted into β-Sn whose surface was mechanically polished before implantation. The spectra have been measured with a $CaSnO_3$ absorber at 200 K and liquid-nitrogen temperature.

$-1.5\%-+0.5\%$ for the case of ^{119}Sn. In the following we use Eq. (2) instead of Eq. (1). Since the absorber used in the present measurements is sufficiently thin (~ 1 mg/cm^2 in ^{119}Sn), the absorption areas (I) corresponding to a certain site and observed at two different temperatures T_1 and T_2 are given by the following equations in emission Mössbauer spectroscopy:

$$I(T_1)=CN^a f^a(T_1)N^s f^s(T_1)\ ,$$
$$I(T_2)=CN^a f^a(T_1)N^s f^s(T_2)\ , \tag{3}$$

where N is the number of Mössbauer nuclei per unit volume, C is a constant, and the superscripts a and s denote absorber and source, respectively. It is noted that the absorber was kept at temperature T_1 in all measurements; $T_1=78$ K and $T_2=150$ or 200 K. Equation (3) leads to

$$I(T_1)/I(T_2)=f^s(T_1)/f^s(T_2)\ . \tag{4}$$

TABLE II. Debye temperatures and Debye-Waller factors at room temperature for the source of ^{119}Sb implanted into β-Sn.

Sample		Θ_{expt} (K)	f_{expt} (293 K)
β-Sn[a]	Line 1	156(4)	0.11(2)
	Line 2	142(16)	0.074(73)
	Line 3	154(5)	0.11(2)
	Line 4	327(148)	0.60(10)
β-Sn		145(3)	0.081(17)

[a]The surface was not polished.

From Eqs. (4) and (2), Θ can be obtained as

$$\Theta=\left[\frac{36E_R T_1 T_2(T_2-T_1)}{E_R(T_2-T_1)+6kT_1T_2\ln[I(T_1)/I(T_2)]}\right]^{1/2}\ . \tag{5}$$

The derived values of the Debye temperature and Debye-Waller factor are given in Table II for the case of implantation into β-Sn.

Kagan *et al.*[16] introduced an effective force constant K for characterizing the interaction between the atoms. They used the following expression for the Debye temperature of the monatomic regular crystal: $\Theta_h=C(K/M_h)^{1/2}$, where C is a constant and M_h is the mass of the host atom. If the interaction is unchanged or is changed only slightly when an impurity (implanted atom) is introduced into a metallic matrix, the assumption that the coupling of the impurity atom to the atoms of the host will be characterized by an effective force constant which is equal or close to the effective force constant of the matrix $K\approx\Theta_h^2 M_i$, is permitted. Then the formula

$$\Theta_{eff}=C(K/M_i)^{1/2}=\Theta_h(M_h/M_i)^{1/2}$$

is derived, where M_i is the mas of the impurity atom and Θ_{eff} is the effective Debye temperature. The Debye temperature for a substitutional site determined experimentally may be compared to the value mentioned. The experimentally determined value of $\Theta_{expt}=145\pm3$ K for Sn in β-Sn does not agree with the calculated value of $\Theta_{eff}=199$ K, where, as Θ_h, for β-Sn $\Theta_h=199$ K was used.[17]

2. *Implantation into Y*

The metallic yttrium is very unstable in the air. It is easily oxidized on the surface. The sample whose surface

TABLE III. Results of Mössbauer measurements on ^{119}Sb implanted into Y.

		Line 1			Line 2			Line 3		
Sample	T_{meas} (K)	δ (mm/s)	I (%)	Γ (mm/s)	δ (mm/s)	I (%)	Γ (mm/s)	δ (mm/s)	I (%)	Γ (mm/s)
Y[a]	78				1.86(2)	15.82(26)	2.02(5)			
	150				1.83(3)	11.19(26)	1.94(6)			
Y[b]	78				1.81(5)	7.97(24)	2.80(8)	0.02(8)	2.23(30)	2.08(8)
	150				1.85(6)	5.62(22)	3.09(8)	0.04(7)	2.17(29)	1.88(8)
Y[c]	78	3.47(7)	3.45(30)	2.08(8)	1.75(4)	10.57(31)	2.02(7)	0.36(7)	3.50(33)	1.98(8)

[a]Sufficient polishing before implantation.
[b]Insufficient polishing before implantation.
[c]After annealing of 440 °C for 40 min using the same source as that of b.

was mechanically polished very well indicated mostly a single-line spectrum as shown in Fig. 4(a). However, an oxide line was also observed when the polishing was not sufficient [Fig. 4(b)]. A line at $\delta = 1.86$ mm/s may be attributed to substitutional sites. A line at zero velocity in the spectrum [Fig. 4(b)] is due to the fraction of the implanted atoms stopped in the oxide layer. The parameters derived from measured spectra are summarized in Table III. The effective Debye temperature determined from the line at $\delta = 1.86$ mm/s is $\Theta_{expt} = 214 \pm 22$ K.

The thermal-annealing experiment with a temperature of 440 °C for 40 min in an argon atmosphere brought about a considerable broadening in the spectral shape. The observed spectrum (curve *c*) in Fig. 4 may be decomposed into three absorption peaks: $\delta \approx 0$ mm/s, $\delta = 1.75$ mm/s, and $\delta = 3.47$ mm/s. The line in the vicinity of zero velocity might be attributed to a defect site. Concerning the line at $\delta = 3.47$ mm/s, no definite assignment can be made.

3. *Implantation into Pb*

Similarly, in the case of yttrium, the surface of the lead metallic foil tends to be oxidized quickly in the air. The Mössbauer spectrum in this case was rather complex.

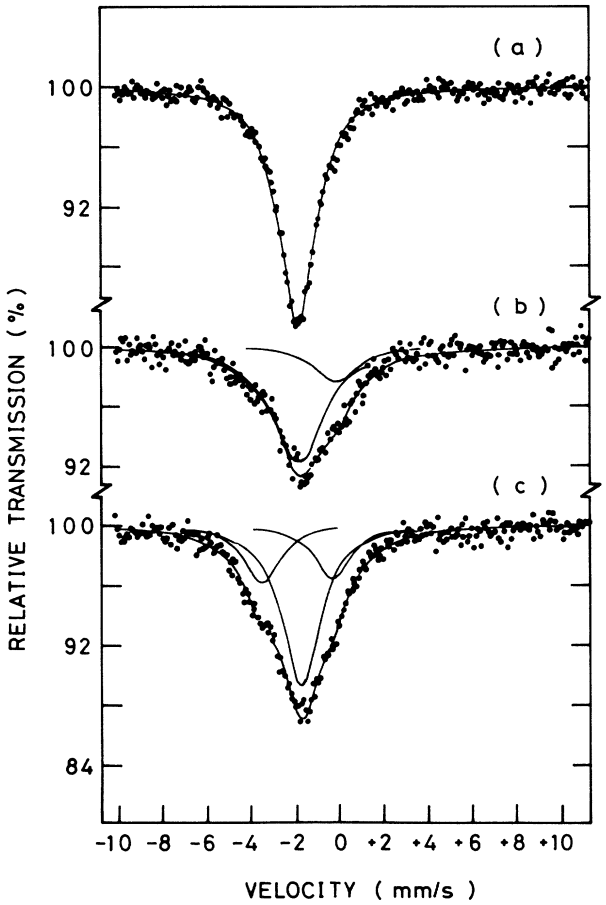

FIG. 4. Mössbauer spectra obtained from sources of ^{119}Sb implanted into Y with a $CaSnO_3$ absorber at liquid-nitrogen temperature. (a) Sufficient polishing before implantation; (b) insufficient polishing before implantation; (c) after annealing of 440 °C for 40 min using the source as same as that of (b).

Two Mössbauer spectra measured at liquid-nitrogen temperature with an annealing at 200 °C for 15 min and without annealing are shown in Fig. 5. It seems that the spectral shape was not affected by the annealing in this case, although some components were slightly different. In the decomposition of these spectra with poor statistics, the information on the number of lines from previous Mössbauer studies was used. Fortunately, since the data from published works on diffused ^{119m}Sn in Pb (Ref. 10) and on implanted ^{119m}Sn in Pb (Ref. 3) were available, by introducing the possible line positions from them, these spectra have been decomposed into five lines with positions at the vicinity of 0, 0.7, 2, 3, and 4 mm/s. In the actual spectral analysis, the oxide line (0 mm/s) and a line at $\delta = 3.1$ mm/s, which is attributed to substitutional tin from the data of diffused ^{119m}Sn in Pb,[10] have been loosely fixed in positions, and all linewidths have been also loosely fixed to an average value for slightly broadened lines (1.9 mm/s). The Mössbauer parameters analyzed with these conditions are listed in Table IV. The effective Debye temperature deduced for the line at $\delta = 3.13$ mm/s, which was assigned as a substitutional tin, $\Theta_{expt} = 129 \pm 7$ K, is close to the value calculated according to the method mentioned in Sec. III A 1, $\Theta_{eff} = 138$ K. In this case $\Theta_h = 105$ K was used for the Debye temperature of the host, i.e., lead. In addition, for the lines found

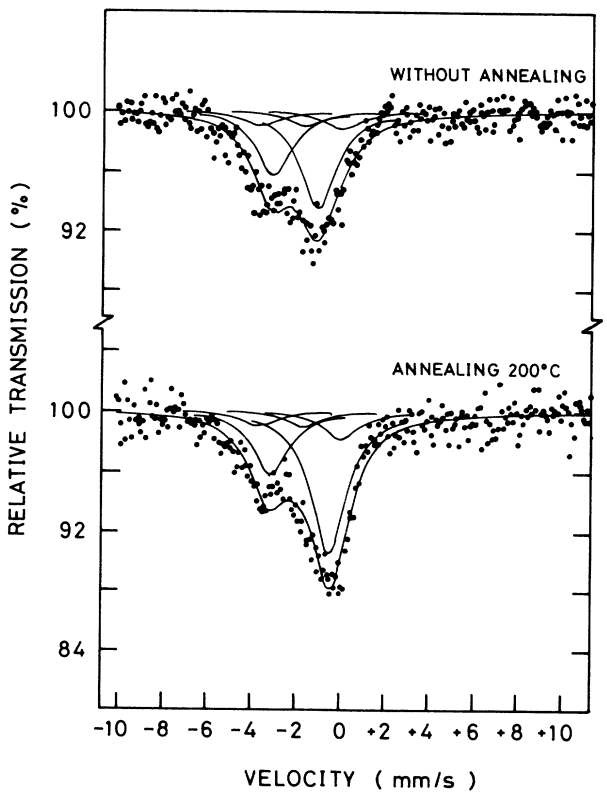

FIG. 5. Mössbauer spectra obtained from the source of ^{119}Sb implanted into Pb with a $CaSnO_2$ absorber at liquid-nitrogen temperature. The spectra have been measured with annealing at 200 °C and without annealing.

at $\delta=1.7$ and 3.7 mm/s, since the Debye temperature for these lines (170 K) indicated a similar value to that observed in the case of the oxide layer on β-Sn ($\sim$155 K), it is considered that these two lines form a quadrupole doublet. Moreover, the Mössbauer parameters of this quadrupole doublet whose splitting and isomer shift are $\Delta=2$ mm/s and $\delta=2.7$ mm/s, respectively, are in good agreement with the values of SnO found in the literature.[7-9] Therefore, two lines at $\delta=1.7$ and 3.7 mm/s may be attributable to the SnO-like species in oxide layers. A line at $\delta=0.5$ mm/s may be attributed to a defect site.

4. *Implantation into Au, Pt, and Al*

In Fig. 6 measured Mössbauer spectra of ^{119}Sb implantations into Au, Pt, and Al are shown. These are fitted with a single resonance line, although in the case of the Al host the existence of an oxide layer was indicated, that is, a weak line at zero velocity was observed in the spectrum. In most cases slightly broadened lines were found compared with the case of β-Sn. In the case of the implantation into the Pt host, a minor component ($\delta=3.2$ mm/s) which might have originated from a certain defect structure was observed before annealing. However, it

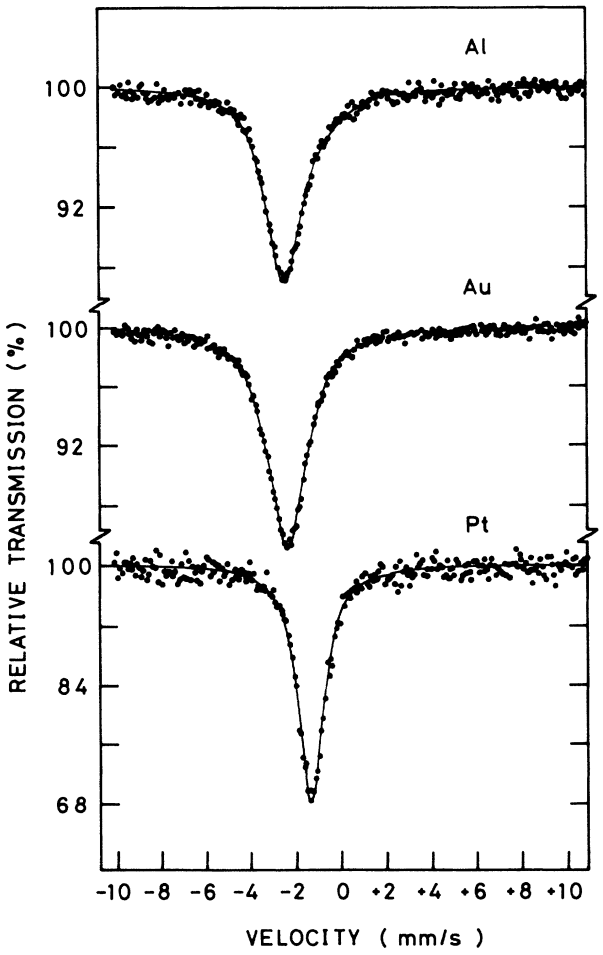

FIG. 6. Mössbauer spectra obtained from sources of ^{119}Sb implanted into Al, Au, and Pt metallic hosts with a $CaSnO_2$ absorber at liquid-nitrogen temperature.

TABLE IV. Results of Mössbauer measurements on ^{119}Sb implanted into Pb.

			Line 1			Line 2			Line 3			Line 4			Line 5		
	Sample	T_{meas} (K)	δ (mm/s)	I (%)	Γ (mm/s)	δ (mm/s)	I (%)	Γ (mm/s)	δ (mm/s)	I (%)	Γ (mm/s)	δ (mm/s)	I (%)	Γ (mm/s)	δ (mm/s)	I (%)	Γ (mm/s)
1	No anneal.	78	3.74(8)	0.99(10)	1.89(9)	3.25(6)	4.17(17)	1.98(8)	1.70(8)	0.99(10)	1.88(9)	1.13(5)	6.42(17)	1.90(7)	0.04(8)	1.16(10)	1.86(9)
	Anneal. 200 °C	78	3.73(9)	0.96(10)	1.88(9)	3.27(7)	3.94(17)	1.97(9)	1.67(9)	1.02(10)	1.87(9)	0.52(4)	9.42(18)	1.93(7)	0.03(9)	1.87(10)	1.84(9)
	Anneal. 200 °C	150	3.70(9)	0.65(9)	1.88(9)	3.14(8)	1.89(9)	1.95(8)	1.69(9)	0.66(10)	1.89(9)	0.53(5)	5.13(17)	1.87(8)	0.03(8)	1.54(10)	1.86(9)
2	No anneal.	78	3.68(12)	0.92(14)	1.85(13)	3.18(9)	4.17(25)	1.82(12)	1.68(12)	0.94(14)	1.86(13)	0.75(7)	6.76(26)	1.80(11)	0.01(10)	3.21(26)	1.74(12)
	Anneal. 200 °C	78	3.69(9)	0.26(1)	1.89(9)	3.19(7)	3.55(16)	2.02(8)	1.71(9)	0.26(1)	1.89(9)	0.77(5)	5.56(17)	2.10(8)	0.02(7)	2.66(17)	1.90(8)
	Anneal. 200 °C	200	3.69(12)	0.10(1)	1.90(12)	3.14(11)	0.90(13)	2.01(12)	1.71(12)	0.10(1)	1.89(12)	0.83(10)	2.63(22)	2.10(11)	0.04(10)	2.68(23)	1.98(11)

TABLE V. Results of Mössbauer measurements on ^{119}Sb implanted into Pt, Al, and Au.

Host	T_{meas} (K)	Line 1 δ (mm/s)	Line 1 I (%)	Line 1 Γ (mm/s)	Line 2 δ (mm/s)	Line 2 I (%)	Line 2 Γ (mm/s)
Pt	78	1.40(2)	19.59(25)	2.20(4)			
	150	1.38(2)	15.71(32)	2.12(6)			
Al	78	2.36(2)	12.83(26)	2.00(5)	0.01(9)	0.41(10)	1.90(9)
	150	2.33(4)	7.61(24)	2.01(7)	0.00(9)	0.40(10)	1.91(9)
Au	78	2.25(2)	14.72(33)	2.03(6)			
	150	2.22(3)	10.14(24)	2.04(6)			

vanished after annealing at 900 °C for 30 min. The results for these measurements are given in Table V. When compared with the data from samples prepared by the diffusion technique (Au,Pt),[10] the present results agree well with them. In addition, the present results seem to be in reasonable agreement with the data[3] reported for the implantations of ^{119m}Sn atoms into Au and Pt. Therefore, the observed lines are attributed to substitutional sites in the lattices. However, a striking difference was observed in the spectral shape for the Al host. Details of this difference will be discussed in Sec. III B.

B. Behavior of the isomer shift in metallic hosts

In order to understand the behavior of the isomer shift of ^{119}Sb introduced as an impurity in various metallic matrices, several attempts have been made. Bryukhanov *et al.*[10] first described the correlation between the Debye force constant of the host lattice and the isomer shift. It was found that an increase in the force constant between the host atoms corresponds to a decrease in the *s*-electron density localized at the tin impurity atom, i.e., in the case of ^{119}Sn a decrease in the value of the isomer shift.

In the Debye model, the force constant between two neighboring atoms is given by $K=\text{const}\Theta_D^2 M$, where Θ_D is the Debye temperature of the material and M is the mass of the atom. Upon introduction of a substitutional impurity atom into the lattice, the effective force constant between the host and the impurity atom is expected to be different from the force constant between the host atoms. In an earlier study,[10] however, it was reasonably assumed that the changes between impurity-host and host-host force constants are small. Actually, from a comparison of the experimentally determined Debye temperature Θ_{expt} for a substitutional site, and the values Θ_{eff} calculated from a model of mass defect mentioned in Sec. III A 1, as shown in Table VI, Θ_{expt} is lower than Θ_{eff} for all hosts, and this simple model seems to be insufficient in the present case. Moreover, it would be seem that these differences indicatively mean that significant changes of the force constants might occur for many cases. If our attention is focused on a comparison between the force constants and isomer shifts, a linear relation is found only in terms of the parameter $\Theta_D^2 M$ which is proportional to the host-host force constant. Figure 7 shows a correlation between the measured isomer shifts for substitutional sites and the force constants of the host materials which are calculated from the Debye model. No linear relation was found between the isomer shifts and the impurity-host force constants. The reason why the isomer shift is not correlated with the impurity-host force constant, but is correlated with the host-host force constant is not clear. It is considered, however, that there might be a possibility of the 3*d* electrons of the impurity atom having an influence on the impurity-host force constant. The 3*d* electrons have little influence on the isomer shift, but may behave effectively in the dynamical interactions be-

TABLE VI. Measured and calculated Debye temperatures for the impurity atoms of tin in various metallic materials. Here, $\Theta_{eff}=\Theta_D(M_h/M_t)^{1/2}$ (see the text).

Host	Θ_{expt} (K)	Θ_{eff} (K)	Θ_D (K)
Pb	129(7)	138	105
β-Sn	145(3)	199	199
Au	180(8)	212	165
Y	214(22)	242	280
Pt	212(9)	307	240
Al	153(6)	204	428

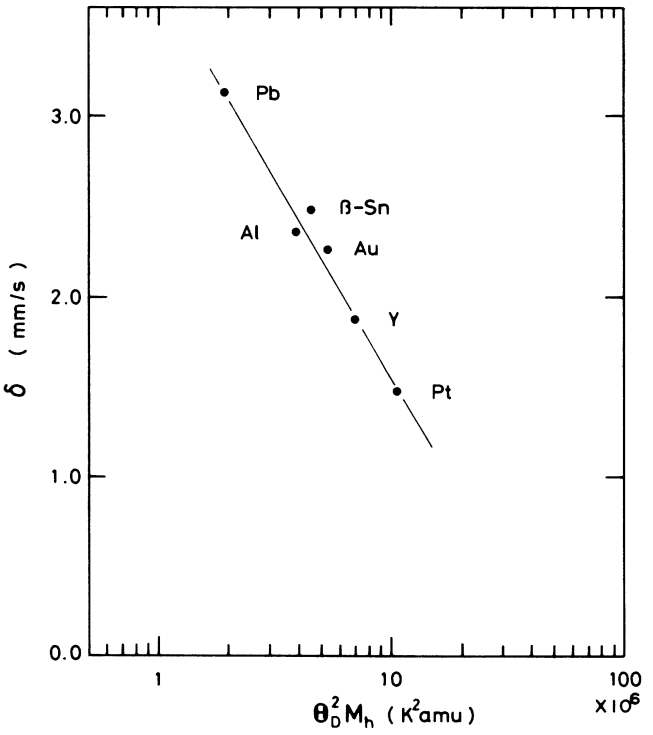

FIG. 7. Correlation between the isomer shift and the Debye force constant of the host for tin in various metals.

tween adjacent atoms. A similar trend to this correlation was observed for the data reported by Bryukhanov *et al.*[10] and Nylansted Larsen *et al.*[3]

Delyagin[18] has reported that a correlation exists between a macroscopic parameter, i.e., matrix compressibility and the isomer shift. With a similar approach to this, parametrizing the physical properties of host materials, namely, the metallic bond radius and the atomic volume, the correlations between these properties and the isomer shift of ^{119}Sb impurities in various matrices are indicated here. Figure 8 shows a correlation between the metallic bond radius for the host matrix and the isomer shift. Here, other data found in the literature are also plotted together with the present data. There is clearly a linear relationship except for the matrices of Ni, Co, Cu, and Y. Since the isomer shifts of tin are predominantly determined by *s* electrons, the observed correlation indicates that the interaction between impurity atoms and host atoms to a considerable extent is by electrons of *s* character. In this respect, for Ni, Co, and Cu which belong to the transition elements, it is likely that *d* electrons contribute considerably to the interaction with the tin impurity atoms. In Fig. 9 a similar correlation between the atomic volume and the isomer shift is depicted. In this figure Ni, Co, Cu, and Y are found to be out of the correlations. For the case of yttrium, plots in both Figs. 8 and 9 obviously deviate from the drawn curves. Although no definite conclusions can be drawn at this stage, the following speculation can be made: not the site having the isomer shift of $\delta = 1.86$ mm/s, but the site having the isomer shift of $\delta = 3.74$ mm/s may be the substitutional position for the implanted atoms in the Y host; therefore, yttrium in Figs. 8 and 9 will be found on the lines. On the other hand, however, this speculation is not consistent with the correlation observed in Fig. 7. The tendency observed in Figs. 7, 8, and 9, in which the curves shown in the figures are a guide to the eye to show the trend of the correlation, is explained qualitatively by using the theoretical descriptions[19–22] for the compression effect, the size effect or, the electronic charge transfer.

The problem of the site assignment in the implantation into metals is rather complicated as defect association can occur. A quadrupole doublet at $\delta = 2.7$ mm/s, which was often observed in several spectra, can be due to the association of one vacancy to a substitutional tin atom according to Weyer *et al.*[3,23,24] Compared to tin atoms without vacancy association, the Debye-Waller factor of the impurity atoms will become lower for this configurations, since one of the bond atoms is missing. A low symmetry for a vacancy-associated substitutional tin site brings about a quadrupole splitting of the Mössbauer

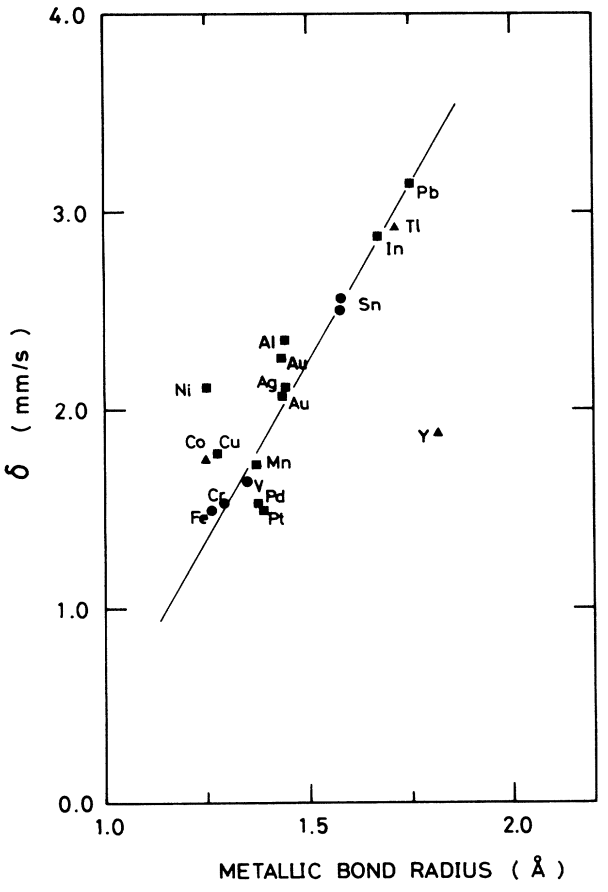

FIG. 8. Correlation between the isomer shift and the metallic bond radius in various metals. ■: fcc; ●: bcc; ▲: hcp.

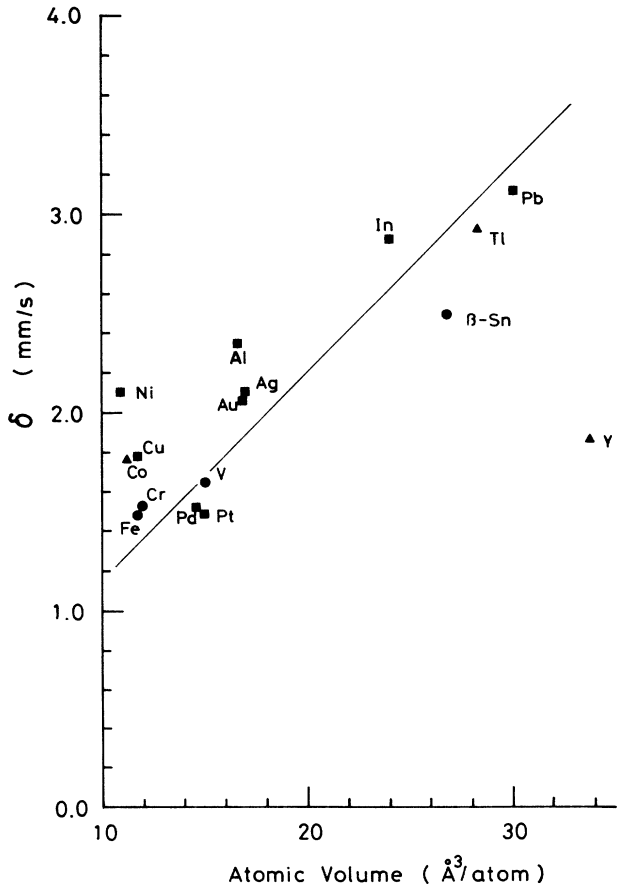

FIG. 9. Correlation between the isomer shift and the atomic volume in various metals. ■: fcc; ●: bcc; ▲: hcp.

line due to the occurrence of an electric field gradient at the tin site.

C. Comparison between ^{119}Sb and ^{119m}Sn implantations

The possibility of influences of the nuclear decay characteristics preceding the emission of the Mössbauer γ rays on the behavior of the implanted atoms were considered in this section, comparing the present data with previous ones obtained in the ^{119m}Sn implantations.[3,4,11] The electron-capture (EC) decay brings about the conversion of ^{119}Sb into ^{119}Sn in the 23.87-keV first excited state with emission of a neutrino, leaving a hole in an inner shell of the tin atom. The Auger process following the EC decay will bring about a nonequilibrium highly charged state of the tin atom. The charge neutralization of this state can be expected to be rather rapid in the solid (less than 10^{-12} s).[25] Therefore, these processes can be assumed to occur within times much shorter than the lifetime (2.6×10^{-8} s) of the Mössbauer level of ^{119}Sn. On the other hand, the ^{119m}Sn mostly decays to the Mössbauer level by internal conversion of the 65-keV $M4$ transition. In the internal conversion of ^{119m}Sn, inner-shell electrons will be converted with a high probability and the electron hole thus created is immediately filled through the emission of characteristic x rays or the Auger process. As a result, an atom with a highly positive charge will be left as well as in the case of the EC decay. In this situation, however, the effects may not be exactly the same, because in the case of ^{119}Sb, the whole electron shells have to be rearranged due to the sudden change of the nuclear charge caused by EC decay. In both cases, since the decaying atoms have reached the electronic configuration of Sn atoms long before the Mössbauer γ ray is emitted, the recorded Mössbauer spectrum is considered to have originated from the electronic configuration of tin.

The recoil energy associated with the neutrino, Auger electrons, and x rays following the EC decay of ^{119}Sb, is estimated to be 1.4, 0.14, and 0.004 eV, respectively.[26] Since the displacement energy of an atom from its substitutional site is about 25–50 eV,[27] which is much larger than the recoil energy, the ^{119}Sn atoms can be expected to stay in the substitutional site of the parent atoms. However, the atoms being in nonsubstitutional sites might be displaced because they may have lower displacement energies.

In the comparison of the present results with those obtained previously from the ^{119m}Sn implantations, no apparent difference was observed between both cases for the implantations into β-Sn, Pt, and Au hosts, that is, their isomer shifts coincided with each other within the limits of experimental error and all of them indicated a single resonance line. It seems to be the same implantation behavior for both Sn and Sb in these metals and the occupied positions, which may be substitutional sites, seem to be stable during the decay as expected from the aforementioned discussions.

On the other hand, a different behavior was observed for the implantations into Al and Pb. In our result for ^{119}Sb in Al, most of the ^{119}Sb atoms occupied the substitutional site ($\delta=2.36$ mm/s) except for some in oxide layers, whereas a more complex spectrum was observed by Nylansted Larsen *et al.*[3] after ^{119m}Sn implantation into Al. In addition, the data obtained by Petersen *et al.*[28] for ^{119}Sb implanted in Al revealed the existence of two or three emission lines. Although no solid argument can be made in this stage for this difference, it may depend on the different implantation energies, i.e., 20 keV in the present work and 60–80 keV in previous observations, which may consequently bring about different radiation damage during the implantation process. For the case of Pb, similar spectra were observed in both the ^{119}Sb and ^{119m}Sn cases. However, the site populations of the implanted atoms differ from each other as shown in Fig. 10(b). The most remarkable difference is in the line around 0.6 mm/s. In contrast with the case of ^{119m}Sn, the site population of this line for the ^{119}Sb implantation was rather large, whereas the populations of the substitutional site at $\delta=3.1$ mm/s are comparable. It is considered that this difference is also due to the different implantation energy rather than to aftereffects of the EC decay which are extremely unlikely in metallic hosts. Nylansted Larsen *et al.* suggested that the line around 2 mm/s might be due to clusters of Sn, because the isomer shift ($\delta=1.9$ mm/s) and recoilless fraction (f) for this line are very close to those for α-Sn ($\delta=2.03$ mm/s, $f=0.14$). For the interpretation of this line, however, it seems to be more reasonable that the lines 1.7 and 3.7 mm/s form a quadrupole doublet. Because the implantation dose in our ^{119}Sb case is lower than that of their ^{119m}Sn experiment by 2 or 3 orders of magnitude and no

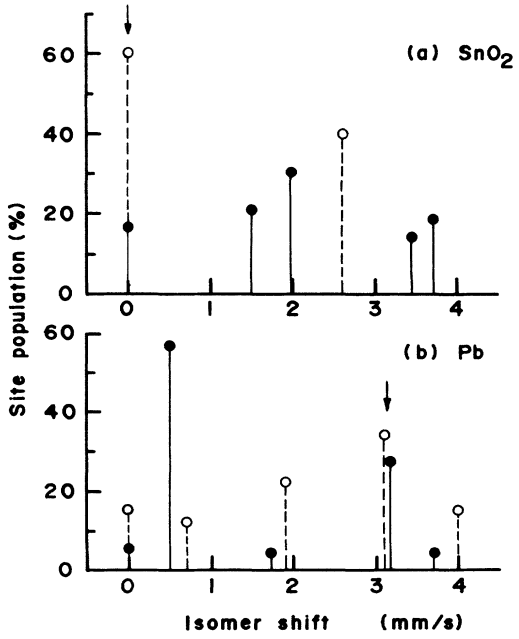

FIG. 10. Site populations of the implanted ^{119}Sb (closed circle) and ^{119m}Sn (open circle) atoms into (a) SnO_2 and (b) Pb hosts. The ^{119m}Sn data were taken from Ref. 11 for tin and from Ref. 3 for lead.

contamination of stable Sn occurs, the cluster formation can be hardly considered in the present case.

It is also interesting to compare our previous result[2] with that reported by Bocquet *et al.*[11] who implanted ^{119m}Sn into SnO_2. Their result shows a singlet corresponding to the Sn(IV) state and only one doublet corresponding to the Sn(II) state, although we decomposed into a singlet and a pair of doublets. The site population of 60% at $\delta=0$ mm /s, in which we are not certain whether they have taken into account the recoilless fractions, is much larger in their case than in our result as shown in Fig. 10(a). This difference may be caused by the difference in the decay characteristics, taking into consideration a preferential stabilization of the implanted atoms in the isoelectronic state with the Sn atoms in the matrix. Ambe *et al.*[26] suggested the importance of the valence state of the cations in the matrix in determining the final valence state of ^{119}Sn.

D. Lattice-dynamical analysis of Mössbauer experiments

One of the unique applications of Mössbauer spectroscopy is the investigation of the fundamental vibronic state of a substitutional impurity in a host-crystal lattice. Among the parameters obtained from Mössbauer spectroscopy, the probability of recoilless γ emission, the so-called Debye-Waller factor (f), measures the mean-squared amplitude of the impurity-lattice vibration. This factor is, in general, expressed as

$$f(T)=\exp(-\kappa^2\langle x^2\rangle_T) , \tag{6}$$

where κ is the wave number of the γ ray and $\langle x^2\rangle_T$ is the mean-squared displacement of the emitting atom in the direction of the emitted γ quantum at temperature T. The mean-squared displacement gives direct information on the lattice vibrations in the case where a Mössbauer atom is a constituent of a metal. On the other hand, the displacement of the peak position in the Mössbauer spectrum observed is called the second-order Doppler shift (SOD) and is given by

$$\delta_{\mathrm{SOD}}=-\langle \dot{x}^2\rangle_T/2c , \tag{7}$$

where $\langle \dot{x}^2\rangle_T$ is the mean-squared velocity of the emitting atom. The SOD data also give information on the lattice vibrations. Through these parameters obtained from Mössbauer measurements, models for the lattice vibrations may be tested. The quantities $\langle x^2\rangle_T$ and $\langle \dot{x}^2\rangle_T$ depend on the impurity-host mass difference and a difference in force constants between the impurity and the host. The interaction between the impurity and the host lattice may cause a change in the vibrational amplitude of the impurity as compared with the host atoms.

Using the Mannheim model,[29] which at present provides the most practical and physically meaningful theoretical framework for an internally consistent method of analysis of Mössbauer lattice dynamics experiments in cubic metals, the force-constant ratio A/A' can be determined by the relation derived by Grow *et al.*:[30]

$$A/A'=(1+(\beta_{-2})^{-2}\{[\mu'(-2)/\mu(-2)](M/M'-1\}) , \tag{8}$$

where $\mu(n)$ and $\mu'(n)$ are the nth moments of the frequency-distribution function for the host and the impurity, respectively, which are expressed via the phonon density-of-states function $G(\omega)$ of the pure-host material and the corresponding function for the impurity $G'(\omega)$. Moment ratios β_n are defined by

$$\beta_n=[\mu(+2)]^{n/2}/\mu(n) . \tag{9}$$

Formula (8) can be rewritten in the terms of Debye temperatures using the relations,

$$\mu(n)=\frac{3}{n+3}\left[\frac{k}{\hbar}\right]^n[\Theta_D(n)]^n ,$$
$$\mu'(n)=\frac{3}{n+3}\left[\frac{k}{\hbar}\right]^n[\Theta'_D(n)]^n . \tag{10}$$

Then, formula (8) is rewritten in the form

$$A/A'=(1+(\beta_{-2})^{-1}\{[\Theta_D(-2)/\Theta'_D(-2)]^2\times(M/M')-1\}) , \tag{11}$$

where $\Theta_D(-2)$ and β_{-2} are derived from Eqs. (9) and (10) with the help of $\mu(+2)$ calculated by Grow *et al.* using data from an appropriate phonon-distribution function $G(\omega)$, based on neutron-dispersion data. $\Theta'_D(-2)$ is the Debye temperature obtained experimentally in the high-temperature Mössbauer fraction measurements. Table VII gives the data used for the calculation of the force-constant ratios together with the result. The relation between the force-constant ratios are thus obtained, and the ^{119}Sn isomer shift is displayed in Fig. 11. For a comparison, the force-constant ratios derived from other formulas, based on the Einstein-Debye model[31] and the

TABLE VII. Host-impurity force-constant ratios from Mössbauer fraction measurements for the ^{119}Sn impurity in four fcc metals and data used for the calculations. The impurity values are denoted by the primes.

Host	M/M'	β_{-2}	$\Theta(-2)$ (K)	$\Theta'(-2)$ (K)	A/A'^{a}	A/A'^{b}	γ/γ'^{c}
Al	0.227	0.556	405	153(6)	2.06	1.87	1.59
Pt	1.64	0.506	236	212(9)	3.12	2.58	2.07
Au	1.66	1.443	164	180(8)	1.86	1.56	1.38
Pb	1.74	0.491	88	129(7)	0.61	0.72	0.81

[a] $A/A'=(1+(\beta_{-2})^{-1}\{[\Theta(-2)/\Theta'(-2)]^2(M/M')-1\})$.
[b] $A/A'=(1+(0.675)^{-1}\{[\Theta(-2)/\Theta'(-2)]^2(M/M')-1\})$.
[c] $\gamma/\gamma'=[\Theta(-2)/\Theta'(-2)]^2(M/M')$.

extended Visscher model by Ohashi and Kobayashi,[32] are also displayed in Fig. 11. Compared with the three force-constant formulas, the same trends are observed between four different fcc metal hosts; however, the spread of the force-constant ratios from the Einstein-Debye, extended Visscher, and Mannheim formulas is larger in that order. The force-constant ratios, except for the lead host, exceed unity. Therefore, this indicates that the impurity-host bonding is significantly weaker than the host-host bonding. It is also shown that the force-constant ratios decrease with decreasing isomer shifts, in other words, decreasing electron density at the nucleus.

According to the discussion in previous studies,[30,33,34] the SOD measurements can, in principle, also be utilized to determine impurity moments, and thus force-constant ratios. As Grow *et al.* have pointed out, this method has two major drawbacks, that is, one is the validity of the assumption that the isomer shift is independent of temperature, and the other is the experimental problem that $\langle \dot{x}^2 \rangle_T$ is relatively insensitive to variation of A/A' for the purpose of obtaining reliable effective host-impurity force-constant ratios. Nevertheless, we attempted the determination of the force-constant ratios from the SOD data obtained from the present work whose data have large experimental errors.

In the case of determining the force-constant ratios from the SOD data, the following relation was derived by Grow *et al.*:[30]

$$A/A' = \{[\mu(+1)/\mu'(+1)](M/M')^{(1/2)+b}\}^{2/[1-b(M'/M)]}, \tag{12}$$

with $b = \frac{1}{2}[\beta_1 - 1]$, where β_1 was calculated by Grow *et al.* Formula (12) can also be rewritten in the terms of Debye temperatures by means of the same manner as mentioned earlier:

$$A/A' = \{[\Theta_D(+1)/\Theta'_D(+1)] \times (M/M')^{(1/2)+b}\}^{2/[1-b(M'/M)]} . \tag{13}$$

Table VIII gives the data necessary for the calculation of the force-constant ratios together with the results. Here, $\Theta'_D(+1)$ is the Debye temperature obtained from the SOD data using the following well-known SOD relation by Maradudin *et al.*:[33]

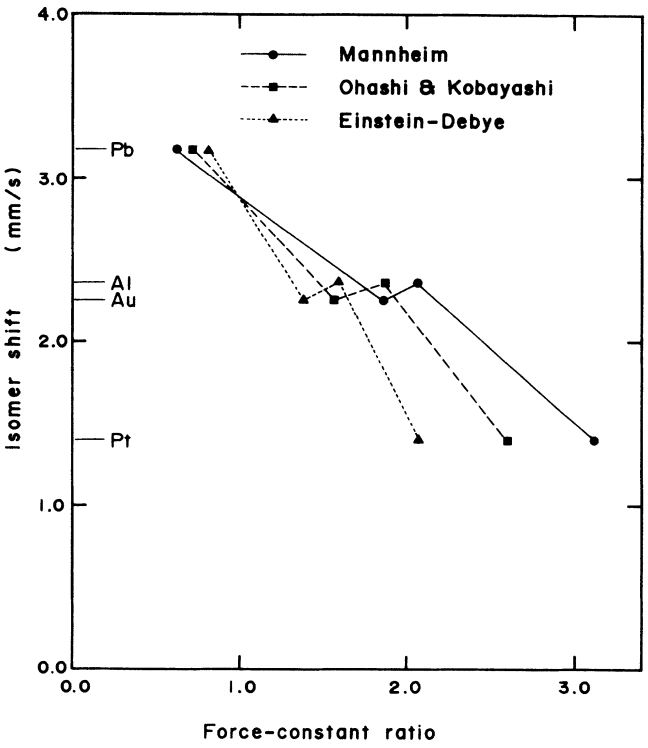

FIG. 11. Force-constant ratios deduced from Mössbauer fraction measurements using three different models for ^{119}Sn impurities in fcc metals against the isomer shift.

$$\mathrm{SOD}(T) = -\frac{3kT}{2Mc}\left[1+\frac{1}{20}\left[\frac{\Theta}{T}\right]^2\right] . \tag{14}$$

In the estimation of $\Theta'_D(+1)$, it was assumed that the isomer shift is independent of temperature. $\Theta_D(+1)$ can be calculated from Eqs. (9) and (10) by using $\mu(+2)$ calculated by Grow *et al.* In Fig. 12 the relation between the force-constant ratios and the isomer shift is depicted for four fcc metal hosts. The force-constant ratios derived from the Einstein-Debye model are also plotted together in Fig. 12. The shift expected from the present measurements at two different temperatures (78 and 150 or 200 K) is to be 0.025 or 0.043 mm/s maximum for a material with very low Debye temperature. These values are the same order of magnitude as the experimental errors. The reason why we attempted to analyze the SOD

TABLE VIII. Host-impurity force-constant ratios from SOD measurements for the ^{119}Sn impurity in four fcc metals and data used for the calculations. The impurity values are denoted by the primes.

Host	M/M'	β_{+1}	b	$\Theta(+1)$ (K)	$\Theta'(+1)$ (K)	A/A'[a]	γ/γ'[b]
Al	0.227	1.046	2.3×10^{-2}	400.5	171.7	1.17	1.23
Pt	1.64	1.050	2.5×10^{-2}	234.8	239.5	1.63	1.58
Au	1.66	1.063	3.15×10^{-2}	178.0	219.3	1.10	1.09
Pb	1.74	1.061	3.05×10^{-2}	92.1	139.3	0.78	0.76

[a] $A/A' = \{[\Theta(+1)/\Theta'(+1)](M/M')^{(1/2)+b}\}^{2/[1-b(M'/M)]}$.
[b] $\gamma/\gamma' = [\Theta(+1)/\Theta'(+1)]^2(M/M')$.

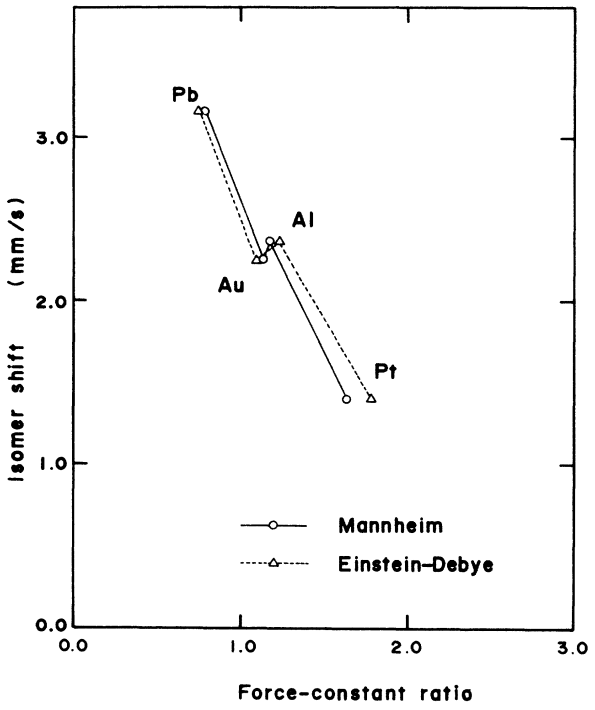

FIG. 12. Force-constant ratios deduced from SOD measurements using two different models for ^{119}Sn impurities in fcc metals against the isomer shift.

data with large experimental uncertainties, is that we examine whether there is any possibility of determining the force-constant ratios from the SOD data or not. As is shown in Fig. 12, the derived force-constant ratios are in reasonable agreement with those derived from the Mössbauer fraction measurements with respect to their trends and magnitude, although the spread of the force-constant ratios may be smaller than that of the fraction measurements. For a comparison between the two different formulas (the Mannheim model and the Einstein-Debye model), as is easily seen, the two formulas are so similar to each other that both results are almost the same. As a concluding remark, it seems that to get accurate SOD data is so difficult in an ordinary experimental situation that reliable force-constant ratios are hardly ever obtained from SOD data.

IV. CONCLUSION

The ion implantation of ^{119}Sb in metals has been studied by Mössbauer spectroscopy on the 23.87-keV transition in ^{119}Sn. The information on the surroundings of the implanted impurity atoms was obtained. The spectra from β-Sn, Au, Pt, and Al have been decomposed into single resonance lines, and these lines were proposed to originate from substitutional impurities judging from their isomer shifts and Debye temperatures. On the other hand, however, complex spectra were observed in the cases of Pb and Y. From the comparison between ^{119}Sb and ^{119m}Sn implantations, observed differences on the spectra from Al and Pb were considered to be due to the difference radiation damage during the different implantation process with different implantation energy. The results of the isomer shifts and Debye temperatures have been analyzed using lattice-dynamic models relating host parameters to the observed impurity parameters. In most cases, except for Pb, the deduced impurity-host force-constant ratios exceeded unity, which indicates that the impurity-host bonding is weaker than the host-host bonding.

ACKNOWLEDGMENTS

The authors would like to thank Professor M. Fujioka for his useful suggestions and encouragement. The cyclotron crew and the Electro-Magnetic Isotope Separator (EMIS) group of the Cyclotron and Radioisotope Center, Tohoku University are greatly acknowledged for their cooperation in the experiments.

*Present address: Department of Chemistry, Faculty of Education, Shinshu University, Nishinagano, Nagano 380, Japan.

[1]H. de Waard, Phys. Scr. **11**, 157 (1975).
[2]H. Muramatsu, T. Miura, H. Nakahara, and M. Fujioka, Radiochem. Radioanal. Lett. **53**, 169 (1982).
[3]A. Nylansted Larsen and G. Weyer, J. Phys. F **9**, 27 (1979).
[4]J. W. Petersen, S. Damgaard, and G. Weyer, J. Phys. F **11**, 487 (1981).
[5]M. Fujioka, T. Shinozuka, E. Tanaka, Y. Arai, S. Hayashibe, and T. Ishimatsu, Nucl. Instrum. Methods. **186**, 121 (1981).
[6]The SALS program (statistical analysis with least-squares fitting) was developed by T. Nakagawa and Y. Oyanagi of the University of Tokyo.
[7]J. K. Lees and P. A. Flinn, J. Chem. Phys. **48**, 882 (1968).
[8]C. G. Davies and J. D. Donaldson, J. Chem. Soc. **A1968**, 946 (1968).
[9]A. J. Boyle, St. P. Bunbury, and C. Edwards, Proc. Phys. Soc. London **79**, 416 (1962).
[10]V. A. Bryukhanov, N. N. Delyagin, and V. S. Shpinel', Zh. Eksp. Teor. Fiz. **47**, 80 (1964) [Sov. Phys.—JETP **20**, 55 (1965)].
[11]J.-P. Bocquet, Y. Y. Chu, O. C. Kistner, M. L. Perlman, and G. T. Emery, Phys. Rev. Lett. **17**, 809 (1968).
[12]T. Miura, Y. Hatsukawa, H. Muramatsu, and H. Nakahara, Nucl. Instrum. Methods B **9**, 123 (1985).
[13]T. Ozawa and Y. Ishida, J. Jap. Inst. Metals **40**, 77 (1976).
[14]P. A. Flinn, *Mössbauer Isomer Shifts* (North-Holland, Amsterdam, 1978), Chap. 9a.
[15]M. Fujioka (unpublished).
[16]Yu. Kagan and Ya. A. Iosilevskiy, Zh. Eksp. Teor. Fiz. **42**, 606 (1962) [Sov. Phys.—JETP **15**, 182 (1962)]; **44**, 284 (1963) [**17**, 195 (1963)].
[17]*American Institute of Physics Handbook*, 3rd ed. (AIP, New York, 1972).
[18]N. N. Deryagin, Fiz. Tverd. Tela (Leningrad) **8**, 3426 (1966) [Sov. Phys.—Solid State **8**, 2748 (1966)].

[19]R. M. Friedman, R. E. Watson, J. Hudis, and M. L. Perlman, Phys. Rev. B **8**, 3569 (1973).
[20]D. L. Williamson, J. H. Dale, W. D. Josephson, and L. D. Roberts, Phys. Rev. B **17**, 1015 (1978).
[21]E. Antoncik, Hyperfine Interact. **11**, 265 (1981).
[22]A. R. Miedema and F. van der Woude, Physica B+C **100B**, 145 (1980).
[23]G. Weyer, A. Nylansted Larsen, N. E. Holm, and H. L. Nielsen, Phys. Rev. B **21**, 4939 (1980).
[24]A. Nylansted Larsen, G. Weyer, and L. Nauver, Phys. Rev. B **21**, 4951 (1980).
[25]H. Frauenfelder, *Annual Review Nuclear Science,* edited by J. G. Beckerley (Annual Reviews, Stanford, Calif., 1953), Vol. 2, p. 129.
[26]F. Ambe, S. Ambe, H. Shoji, and N. Saito, J. Chem. Phys. **60**, 3773 (1974).
[27]H. Bernas, Phys. Scr. **11**, 167 (1975).
[28]J. W. Petersen, S. Damgaard, and G. Weyer, J. Phys. F **11**, 487 (1981).
[29]P. D. Mannheim, Phys. Rev. **165**, 1011 (1968).
[30]J. M. Grow, D. G. Howard, R. H. Nussbaum, and M. Takeo, Phys. Rev. B **17**, 15 (1978).
[31]See for example, Ref. 30.
[32]K. Ohashi and K. Kobayashi, J. Phys. F **5**, 1466 (1975).
[33]A. A. Maradudin, P. A. Flinn, and S. L. Ruby, Phys. Rev. **126**, 9 (1962).
[34]R. M. Housley and F. Hess, Phys. Rev. **146**, 517 (1966).